Quantum localization and electronic transport in covalently functionalized carbon nanotubes

Ghassen Jemaï[1] ⓘ**, Jouda Jemaa Khabthani**[1] ⓘ**, Guy Trambly de Laissardière**[2] ⓘ **and Didier Mayou**[3,4] ⓘ

[1] Laboratoire de Physique de la Matière Condensée, Département de Physique, Faculté des Sciences de Tunis, Université Tunis El Manar, Campus Universitaire, 1060 Tunis, Tunisia
[2] Laboratoire de Physique Théorique et Modélisation, CNRS and Université de Cergy-Pontoise, 95302 Cergy-Pontoise, France
[3] CNRS, Inst NEEL, F-38042 Grenoble, France
[4] Université Grenoble Alpes, Inst NEEL, F-38042 Grenoble, France

E-mail: guy.trambly@u-cergy.fr

CrossMark

Abstract

Carbon nanotubes are of central importance for applications in nano-electronics thanks to their exceptional transport properties. They can be used as sensors, for example in biological applications, provided that they are functionalized to detect specific molecules. Due to their one-dimensional geometry the carbon nanotubes are very sensitive to the phenomenon of Anderson localization and it is therefore essential to know how the functionalization modifies their conduction properties and if they remain good conductors. Here we present a study of the quantum localization induced by functionalization in metallic single walled carbon nanotubes (SWCNT) with circumferences up to 15 nm. We consider resonant and non-resonant adsorbates that represent two types of covalently functionalized groups with strong and moderate scattering properties. The present study provides a detailed analysis of the localization behaviour and shows that the localization length can decrease down to 20–50 nm at concentrations of about 1 percent of adsorbates. On this basis we discuss the possible electronic transport mechanisms which can be either metallic like or insulating like with variable range hopping.

Keywords: carbon nanotube, quantum transport, electronic localization

S Supplementary material for this article is available online

(Some figures may appear in colour only in the online journal)

1. Introduction

Single walled carbon nanotubes (SWCNTs) are quasi-one-dimensional cylindrical shape materials with sp^2 hybridized carbon atoms, that exhibit unique physical and chemical properties. Since their discovery in 1991, they have attracted much attention for their fundamental properties and their wide range of potential applications, such as for energy storage [1, 2], solar cells [3–5], nano-electronics and sensors devices [6, 7].

SWCNT get easily bundled forming agglomeration of nanotubes as a result of the strong Van der Walls energy interaction [8], and because of that it's always challenging to manipulate them efficiently for experiments. Yet surface functionalization allows to overcome this problem since ad-atoms and molecules covalently attached to it's surface can greatly reduce the effect of the strong Van der Walls interaction. The functionalization also allows the compatibility toward other molecules to create new composite materials based on carbon nanotubes [9, 10].

In particular, it has been reported that SWCNT is ideal to create reliable and accurate electrochemical biosensor, faster than conventional ones [2, 6, 11, 12], thanks to its low dimensionality, nanometric size, large surface area, high sensitivity and fast response. The two main components in such device, are the biological recognition element that detects a biological molecule and the transductor that collects a charge transferred from the biological molecule to convert it into an electrical signal unique to a specific detected element. Since a covalent functionalization can drastically alter the electronic properties of carbon nanotubes [13, 14], it can affect the detection process in a biosensor.

Many theoretical analyses of electronic transport in SWCNT have been carried out using different numerical techniques, such as real space Kubo–Greenwood method for bulk systems [15–17], and Laudauer type formalisms for finite systems coupled to leads [14, 18–26]. Most of them discussed the importance of the Anderson localization due to charged defects or local defects such as vacancies, ad-atoms or ad-molecules. However, a global understanding of localization process based on numerical calculations that takes into account the effects of quantum interferences without approximations is still missing. In this paper we investigate these effects for SWCNT of diameter up to 4-5 nm and large concentrations of functionalized sites up to 1 or a few percent. In particular we address the question of the coherent electronic transport in the nanotube and the occurence of localization effect which can diminish the conduction properties of the functionalized nanotube [27–29]. Since strong localization effects are inherent to low dimensional conductors [13, 26] it is important to have a clear description of its effect on these electronic devices. Our approach allows to propose a detailed analysis of the conductivity and its correction due to quantum localization for a wide range of concentrations of resonant and non-resonant defects. It is confirmed that quantum localization is the key to understand the wide variety of transport regimes depending on the nanotube diameter, the adsorbates concentration and the type of functionalization. In particular we show that at low adsorbates concentration the system obeys the Thouless relation, typical of a one-dimensional system, which links the number of conducting channels, the elastic mean-free path and the localization length. The values of these fundamental lengths are estimated for resonant and non-resonant adsorbates with concentration ranging from 0.1% to 4%, which corresponds to different types of applications such as sensors. Yet we show also that these nanotubes can present a variety of other behaviors that emerge at sufficiently high concentration of adsorbates. For example we find that a transition form 1D localization behavior to 2D localization behavior can occur for resonant scatterers at a concentration of the order of 1%. Also, depending on the adsorbate concentration and nanotube diameter we discuss the occurence of a regime of variable range hopping which could possibly be observed at room temperature.

The paper is organized as follows. First section presents the tight-binding model and the basic concepts used to analyze the quantum localization effect on transport. The numerical method to study SWCNT is presented section 2 and in the supplementary material (stacks.iop.org/JPhysCM/32/115301/mmedia). Then we analyze the localization in the cases of carbon nanotube functionalized with non-resonant (section 3) or resonant (section 4) adsorbates with various concentrations in the range of 0.1% to 4%. A discussion is given section 5 about the transport mechanism metallic like or insulating like and in particular the possibility of variable range hopping.

2. Model and methodology

2.1. Modeling resonant and non-resonants adsorbates in SWCNT

A single walled carbon nanotube (SWCNT) is equivalent to a rolled up stripe of a 2D graphene sheet. The orientation of rolling up graphene, is defined by the chiral vector $\vec{C}_h = n\vec{a}_1 + m\vec{a}_2$, where $\vec{a}_1$ and $\vec{a}_2$ are the unit cell vectors of graphene, the n and m are coefficients used to define the chirality of the nanotube. The SWCNT diameter is $d = \frac{C_h}{\pi}$ where $C_h = \left\|\vec{C}_h\right\| = a\sqrt{3(n^2 + m^2 + nm)}$ the circumference of the nanotube, with $a = 0.142$ nm the distance between two neighboring carbon atoms. The ratio between the length and diameter $\frac{L}{d} \sim \left(\frac{\text{length}}{\text{diameter}}\right)$ can be as large as 10^4 to 10^5 [30] and carbon nanotube can be considered as a quasi-one-dimensional nano-structure. In this study the SWCNT has an infinite length which avoids edges effects.

In this paper we consider the metallic zigzag single walled carbon nanotube $(n, 0)$ where the shape of the SWCNT cross section is zigzag and with 'n' is a multiple integer of 3. We took $n = 30$, $n = 60$ and $n = 90$. We show detailed results for $n = 60$ in the article and compare them with the results for $n = 30$ and $n = 90$ that are summarised in the supplementary material.

We study the electronic properties of SWCNT using a first neighbour tight-binding hamiltonian

$$\tilde{H} = -t \sum_{i,j} \left(c_i^\dagger c_j + c_i c_j^\dagger \right), \tag{1}$$

where $c_i^\dagger$ (c_i) is the creation (annihilation) operator. The hopping integral $t = 2.7$ eV allows the electron to hop from an atom site to one of its three first neighbours. We consider that all the onsite energies are the same and they are all set to zero ($\varepsilon_0 = 0$ eV).

When an ad-atom or molecule is attached to the nanotube surface it creates an adsorbate and a covalent bond. This covalent bond is equivalent to taking out a p_z orbital. It has been established that adsorption on top of a carbon atom allows to keep the sp^2 hybridization [31, 32]. Therefore we model adsorption on top of a carbon site by simply removing the corresponding p_z orbital in equation (1). We therefore assume that an adsorbate can be seen as a carbon vacancy present in the SWCNT without disturbing the other carbon atoms positions. Note that an adsorbate is a local defect and produces inter-valley scattering which leads to Anderson localization [33–35].

We consider two types of local defects obtained by removing one isolated p_z orbital or two neighboring p_z orbitals. These two types of defects correspond respectively to resonant and non-resonant adsorbates. Indeed the effect of an isolated local defect is entirely described by an energy dependent T-matrix $T(E)$. Resonant adsorbates are modeled by removing one isolated p_z orbitals and the corresponding T-matrix presents a strong resonance at the charge neutrality point (CNP) creating a peak in the density of states around the CNP. A similar peaks exist in graphene for which $T(E)$ even presents a divergence at the CNP. Non-resonant adsorbates, are modelled by removing two neighbouring orbitals at the same time. In that case the T-matrix varies smoothly with energy and does not show resonance close to the CNP. Therefore no peak appears in the DOS around the CNP. Resonant and non-resonant adsorbates affect differently the electronic transport, and in particular the resonant adsorbates produce a stronger scattering than the non-resonants adsorbates close to the CNP.

2.2. Analysis of quantum localization

Following the real space Kubo–Greenwood method [36–41] for transport properties of electron in the nanotube, we compute $X^2(E,t)$ which is the average square of the quantum spreading along the direction of the nanotube, after a time t and for states at energy E. That method has been also used to study graphene monolayer [42], bilayer [43, 44]. For an electron in a 1D system propagating in a static disordered potential we know that all states are localized and quantum diffusion is limited by the localization length $\xi(E)$. Yet the time evolution of $X^2(E,t)$ contains much information about the localization phenomena. In order to do this analysis we simulate how inelastic scattering affects diffusion and conductivity. At the simplest level the effect of inelastic scattering is described by introducing an inelastic scattering time τ_{ie} and a time of phase coherence of the wave-function τ_Φ. These two times can be different and their relative value can depend on the studied system. In carbon nanotubes it has been argued that τ_Φ can be smaller than τ_{ie} because loss of phase coherence can be due predominantly to long wavelength acoustic modes which have a small effect on τ_{ie} [17]. In the present study we use the relaxation time approximation (RTA) which consist in assuming that the velocity correlation function of the system is destroyed by inelastic scattering and the associated loss of wave-function coherence. In this picture their is no distinction between τ_Φ and τ_{ie}. We therefore introduce a parameter τ_i such that $\tau_i \simeq \tau_{ie} \simeq \tau_\Phi$. Associated to τ_i there is a length scale called the inelastic mean-free path $L_i(E, \tau_i)$ which is the typical propagation length at energy E after a time τ_i (see supplementary material for precise definition). Beyond τ_i the transport regime is diffusive because of the loss of coherence, and the diffusivity is given by $D(E, \tau_i) = \frac{L_i^2(E,\tau_i)}{\tau_i}$. The expression of electrical conductivity becomes

$$\sigma(E_F, \tau_i) = 2e^2 n(E_F) D(E_F, \tau_i),\qquad(2)$$

where $n(E_F)$ is the density of states per unit length (per spin) at the Fermi energy E_F. As shown below the variation of the conductivity $\sigma(E_F, \tau_i)$ with $L_i(E, \tau_i)$ or with τ_i contains essential information about the quantum transport. It allows to extract also the elastic mean-free path $l_e(E)$ and the localization length $\xi(E)$, and will be discussed in detail. For example an important quantity is $\sigma_M(E_F)$ the maximum of the conductivity as a function of $L_i(E, \tau_i)$. In the following $\sigma_M(E_F)$ is named the microscopic conductivity. It corresponds to a situation where the inelastic mean-free path is of the order of the elastic mean-free path so that the effect of quantum localization cannot develop and decrease the conductivity. $\sigma_M(E_F)$ is given in term of the mean-free path $l_e(E)$ by

$$\sigma_M(E_F) = G_0 N_{ch}(E_F) l_e(E_F),\qquad(3)$$

where $G_0 = 2e^2/h$ is the quantum of conductance and $N_{ch}(E) = n(E)/n_0$ is the ratio between the density of states per unit length and per spin $n(E)$ at the energy E and the density of states for one channel $n_0 = 2/hV_G$ where V_G is the velocity in graphene at the CNP. n_0 is half the density of states at the zero energy in the nanotube (there are two conduction channels near $E = 0$ one close to each Dirac point). Therefore $N_{ch}(E)$ is close to the number of channel at the energy E but tends to be higher because the contribution to the density of states of a channel close to its minimum energy (Van Hove singularity) is higher than $n_0 = 2/hV_G$.

3. Electronic transport for non-resonant adsorbates

We investigate the electronic behavior of metallic SWCNT $(60, 0)$ with a large diameter $d = 4.75$ nm and a circumference $C_h = 14.94$ nm, in presence of non-resonant adsorbates. We consider first the low concentration cases (0.1%, 0.2% and 0.4%) (figure 1) and then higher concentrations cases (1%, 2% and 4%) (figure 2).

Figure 1(a) shows the total density of states versus energy. For low energy near the CNP, the DOS is weakly affected by disorder. At larger energy and in particular close to Van Hove singularity (VHS), the modification of the DOS is more important.

Figure 1(b), shows the elastic mean-free path l_e as a function of energy E. l_e is maximum around the CNP energy and decreases by crossing a VHS. It reaches a new maximum in between two successive VHS. Indeed the probability of scattering increases as a function of energy according to the DOS and therefore the mean scattering time and the mean-free path decrease. In addition the new channel that appears at a VHS has a low band velocity. The probability of scattering also increases by increasing the concentration of adsorbates which results in a shorter elastic mean-free path. The results show that l_e is inversely proportional to the concentration of adsorbates, which is in accordance with the Fermi Golden rule.

The microscopic conductivity σ_M versus energy is shown in figure 1(c). This quantity is given by equation (3) and is proportional to the product of results in figures 1(a) and (b). The evolution of σ_M as a function of energy, follows globally the behaviour of l_e as a function of energy. As for the elastic mean-free path the increase of concentration of adsorbates decreases the conductivity σ_M which is inversely proportional
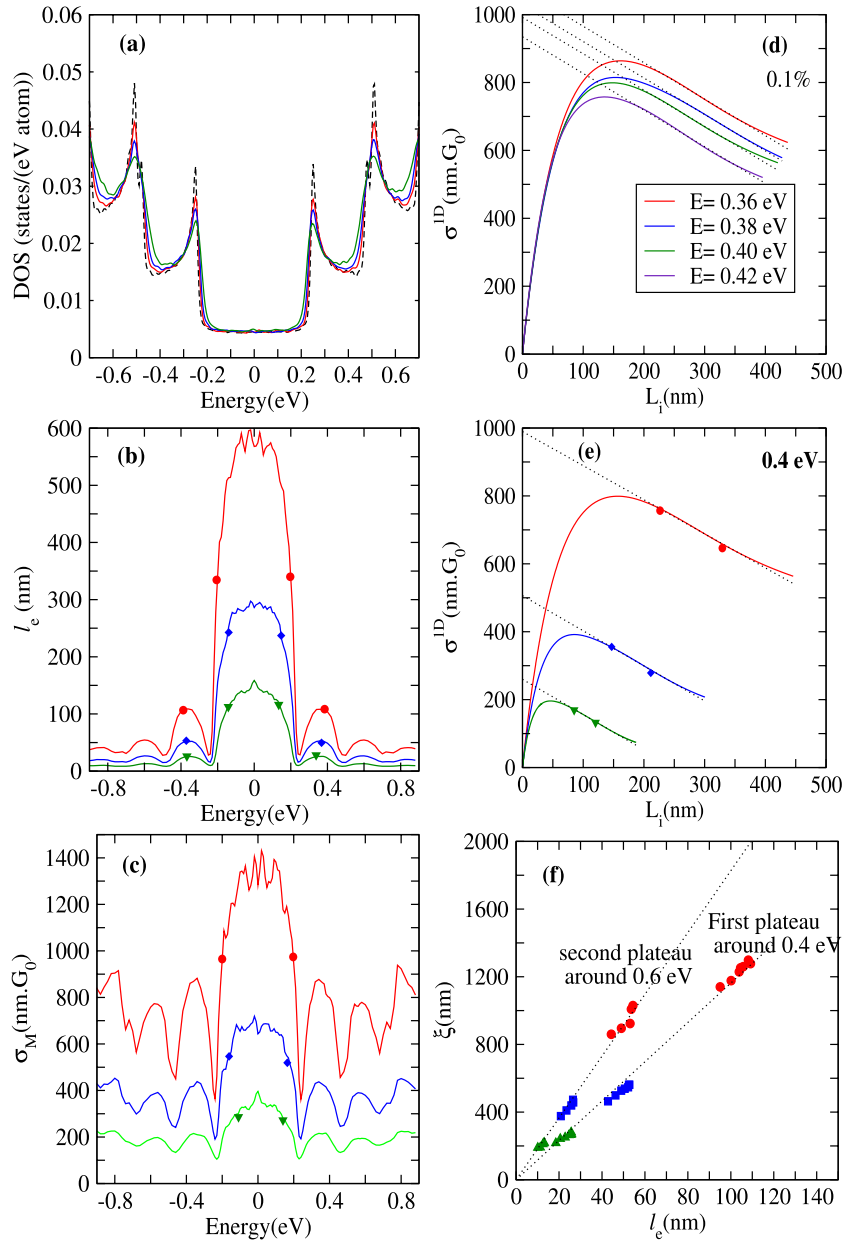
Figure 1. Low concentration of non-resonant adsorbates: 0.1% (red/filled circle), 0.2% (blue/filled square) and 0.4% (green/filled triangle). (a) Density of states versus energy, (b) Elastic mean-free path l_e versus energy, (c) Microscopic conductivity σ_M versus energy, (d) Electronic conductivity σ versus inelastic mean-free path L_i for 0.1% of non-resonant adsorbates, (e) Electronic conductivity σ versus inelastic mean-free path L_i at $E = 0.4$ eV, and (f) Localization length ξ versus elastic mean-free path l_e (Thouless relation).

to the concentration of adsorbates. σ_M is a semi-classical quantity corresponding to the diffusive regime when L_i and l_e are comparable. Thus, it does not depend on the quantum localization effects.

Figures 1(d) and (e) present the electronic conductivity as a function of the inelastic mean-free path. At low L_i, $\sigma(E_F, \tau_i)$ increases in the ballistic regime. Then it reaches its maximum and for large L_i decreases because of Anderson localization. In the localization regime, we find that the conductivity behaves according to the 1D scale dependent conductivity [45] given by

$$\sigma(E_F, L_i) = \sigma_M(E_F) - G_0 (L_i - L_e). \qquad (4)$$

Here L_e is defined as the value of L_i for which the extension of the linear regime crosses the maximum value of $\sigma_M(E_F)$. L_e is expected to be of the order of the elastic mean-free path l_e and indeed we find numerically that $L_e \simeq 2l_e$. The behavior given by equation (4) is consistent with the standard theory of localization in one dimensional conductors [45].

The localization length $\xi(E)$ is defined as the value of L_i for which the extrapolation of equation (4) cancels. Therefore using equation (3) and since $L_e \simeq 2l_e$ one get

$$\xi(E) \simeq (N_{ch}(E) + 2)l_e(E), \qquad (5)$$

where, in this Thouless relation [46], $N_{ch}(E) = n(E)/n_0$. As explained previously $N_{ch}(E)$ is close to the number of channels
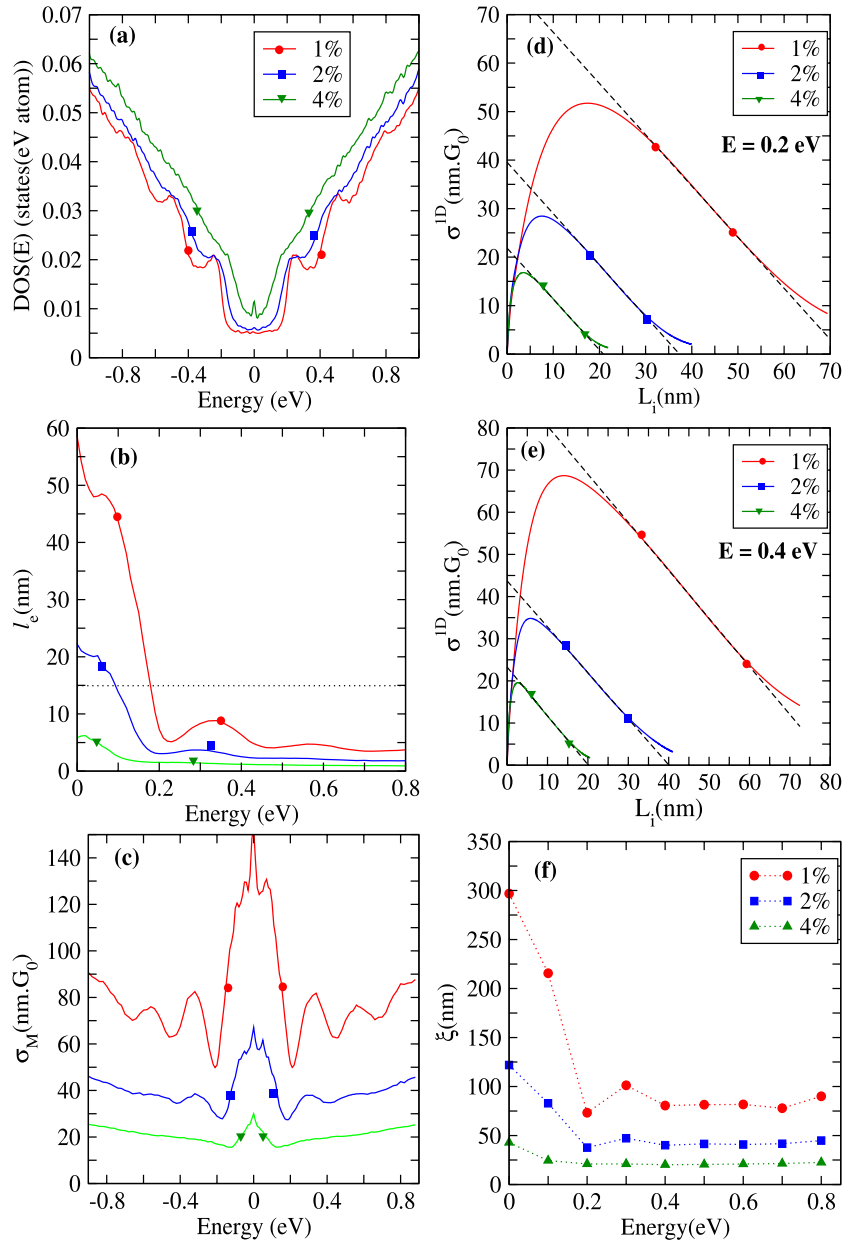
Figure 2. High concentration of non-resonant adsorbates: 1% (red/filled circle), 2% (blue/filled square) and 4% (green/filled triangle). (a) Density of states versus energy, (b) Elastic mean-free path l_e versus energy, (c) Microscopic conductivity per unit surface σ_M/C_h versus energy, (d) Electronic conductivity σ versus inelastic mean-free path L_i at $E = 0.2\,\text{eV}$, (e) Electronic conductivity σ versus inelastic mean-free path L_i at $E = 0.4\,\text{eV}$, and (f) Localization length ξ versus energy.

at the energy E but tends to be higher. As shown in the figure 1(f), the localization length ξ evolves as a linear function of elastic mean-free path l_e as predicted by the Thouless relation with a slope that increases with the number of conduction channels N_{ch}. For the first plateau around 0.4 eV, $N_{\text{ch}} \approx 6$ and $N_{\text{ch}} \approx 10$ for the second plateau around 0.6 eV. These results confirm the accuracy of our numerical calculations.

Figure 2 presents a similar study as figure 1 but for higher concentrations (1%, 2% and 4%), the modification of the DOS by disorder becomes more important and the VHS are smeared out. In addition for the concentration (4%) the density of states is strongly modified even close to the CNP. Despite these differences the variations of $l_e(E)$, $\xi(E)$ and $\sigma_M(E)$ remain similar

and are still inversely proportional to the concentration. The linear variation of conductivity with L_i is also given by equation (4). Note that even at high concentration of non-resonant adsorbates the localization length is allways larger than the circumference of the nanotube $\xi > C_h$ as shown in figure 2(f).

We conclude therefore that for the non-resonant adsorbates the nanotube behaves as a 1D conductor with a relatively small amount of disorder, for which the microscopic conductivity $\sigma_M(E)$ and the elastic mean-free path $l_e(E)$ are obtained from the Fermi golden rule. In addition our results confirm the Thouless relation between the localization length $\xi(E)$, the elastic mean-free path and the number of conduction channels.
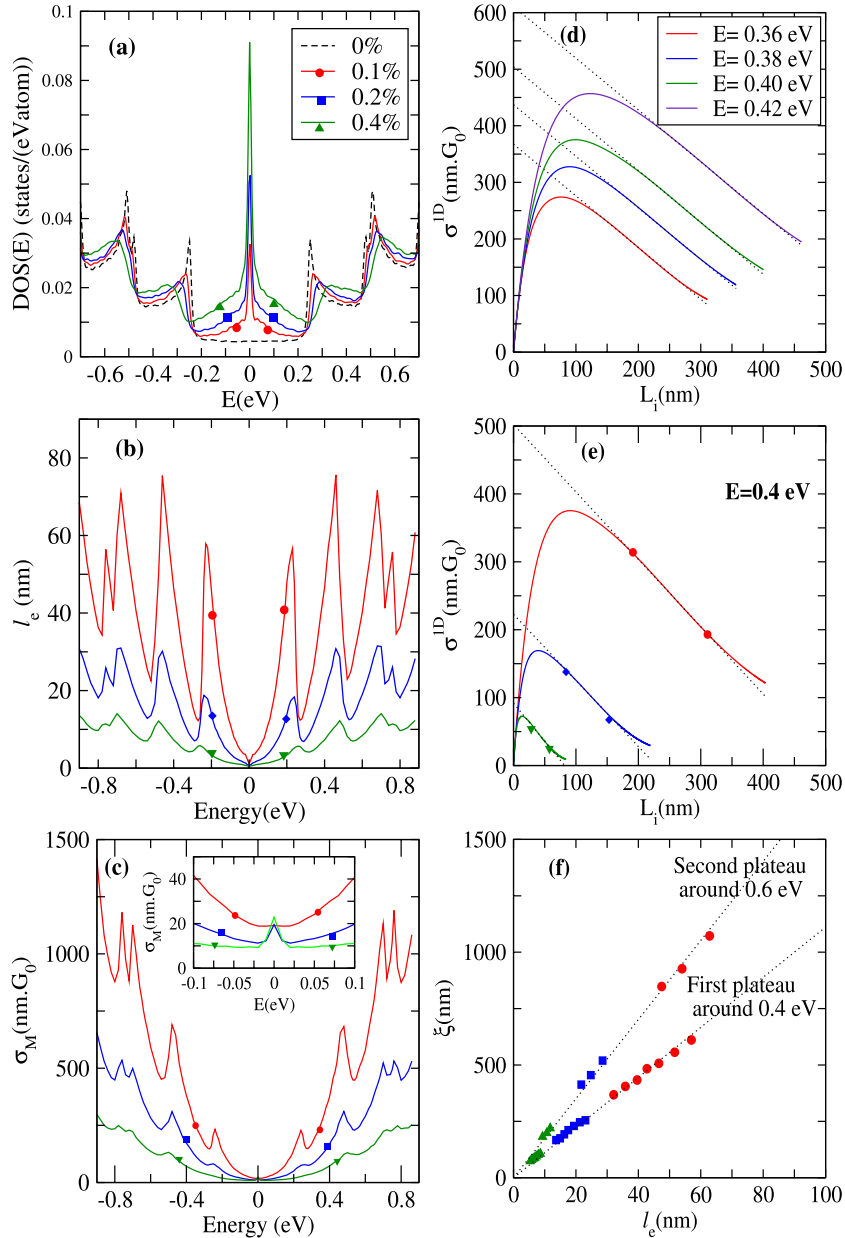
Figure 3. Low concentration of resonant adsorbates: 0.1% (red/filled circle), 0.2% (blue/filled square) and 0.4% (green/filled triangle). (a) Density of states versus energy, (b) Elastic mean-free path l_e versus energy, (c) Microscopic conductivity σ_M versus energy, (d) Electronic conductivity σ versus inelastic mean-free path L_i for 0.1% of resonant adsorbates, (e) Electronic conductivity σ versus inelastic mean-free path L_i at $E = 0.4$ eV, and (f) Localization length ξ versus elastic mean-free path l_e (Thouless relation).
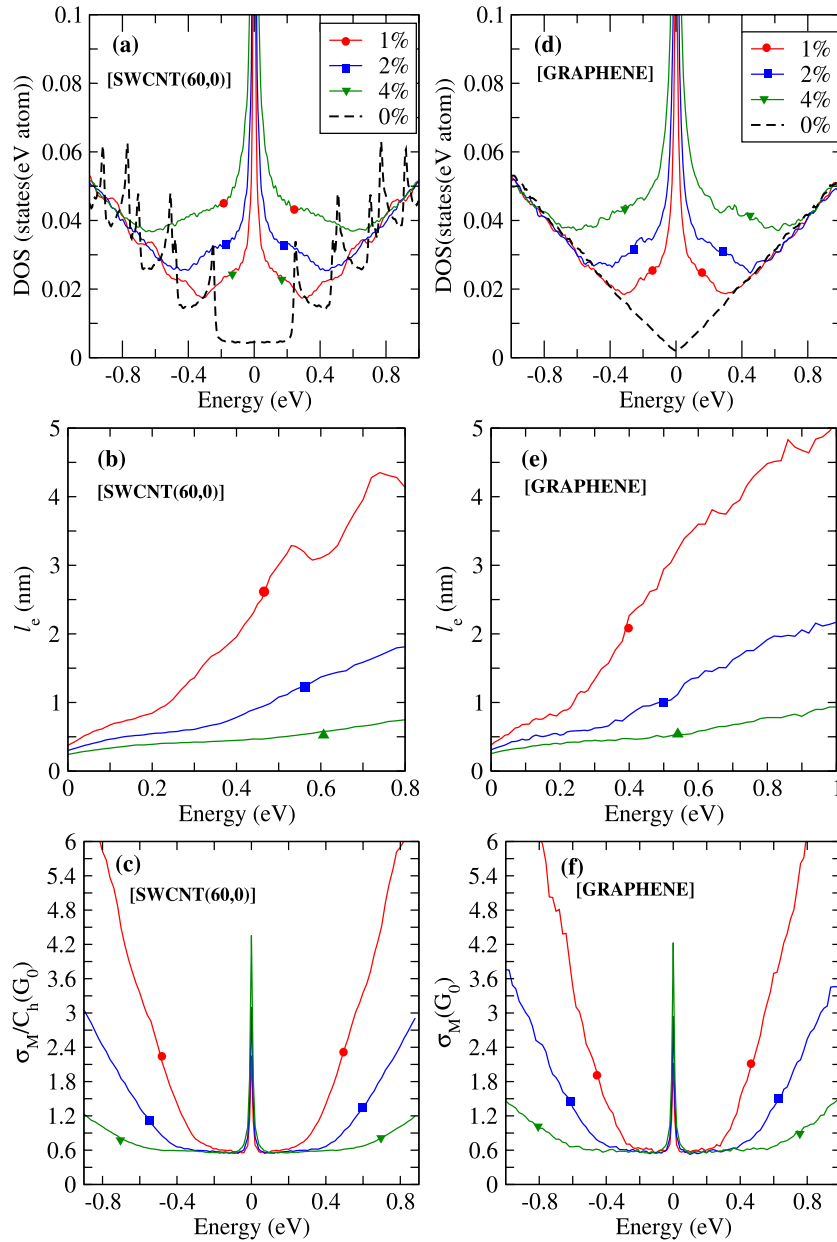
4. Electronic transport for resonant adsorbates

We now investigate the electronic behavior of the metallic SWCNT $(60,0)$ in presence of resonant adsorbates. We consider first the low concentration cases (0.1%, 0.2% and 0.4%) (figure 3) and then higher concentrations cases (1%, 2% and 4%) (figure 4).

In figure 3(a), the density of states versus energy for resonant adsorbates shows more dramatical effects with a pic of resonant states around the Fermi's energy, a shift in the plateau of the DOS for larger energy and the positions and height of the VHS are greatly affected.

For resonants adsorbates as shown in figure 3(b), the mean-free path increases as a function of energy within a plateau

of energy and by crossing a VHS, since the probability of scattering is much higher for low energies close to the resonant states where l_e is at its minimal value. l_e is shown to be always larger than the circumference of the nanotube which confirms that the electronic behavior of SWCNT $(60,0)$ is one dimensional.

The microscopic conductivity σ_M expressed in unit of quantum conductance $G_0 = 2e^2/h$ versus energy is shown in figure 3(c) for low concentration of resonant adsorbates. The increase of concentration of adsorbates decreases the conductivity σ_M. The evolution of σ_M as a function of energy, follows the general behavior of l_e as a function of energy. σ_M is a semi-classical quantity computed in the diffusive regime when L_i and l_e are comparable. Thus, it does not take into account the

Figure 4. A comparative representation of electronic transport properties of SWCNT (60,0) and graphene at high concentration of resonant adsorbates: 1% (red/filled circle), 2% (blue/filled square) and 4% (green/filled triangle). (SWCNT(60,0)) (a) Density of states, (b) Elastic mean-free path l_e, and (c) Microscopic conductivity per unit of surface, σ_M/C_h, versus energy. (GRAPHENE) (d) Density of states, (e) Elastic mean-free path l_e, and (f) Microscopic conductivity σ_M, versus energy.

quantum effects (localization effects). The right column of figure 3 shows the occurence of localization effects similar to those shown for the non-resonant states. This behavior corresponds to the laws of one-dimensional conductors as given by equations (4) and (5).

Figure 4(a), shows that at high concentration of resonant adsorbates (1%, 2% and 4%), the VHS disappear from the density of states around the Fermi's energy, because the effects of electronic scattering is so dramatic to the point that the quantification of the $\vec{k}$ vector in the direction of $\vec{C_h}$ is broken. The new shape of the DOS is actually close to the DOS of graphene shown in figure 4(d).

We can see in figure 4(b) that the elastic mean-free path is much shorter than the circumference C_h, for all energies. As a result, we can expect a transition from one-dimensional towards two-dimensional electronic behavior in a SWCNT induced by increasing the concentration of adsorbates. Indeed if the characteristic lengths are shorter than its circumference the nanotube should behave like a sheet of graphene.

This dimensionality crossover should be identified by investigating the effects on the microscopic conductivity and the scale dependent conductivity. Since the beginning, the electrical conductivity σ is expressed in units of length for one-dimensional system σ^{1D}, we redefine this quantity for a
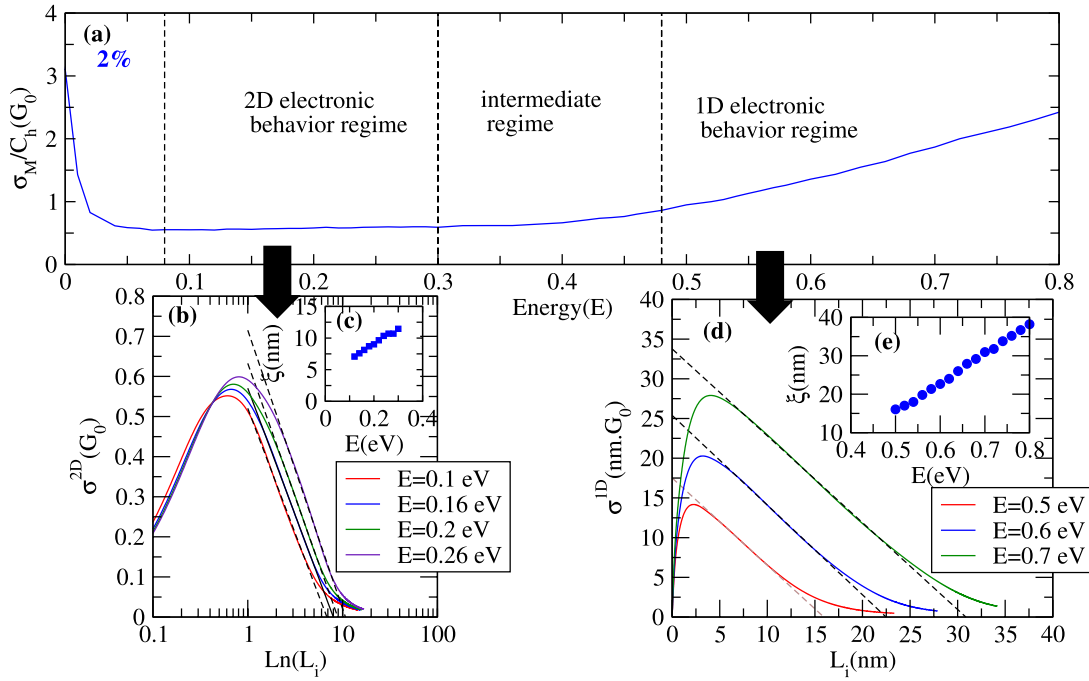
Figure 5. For SWCNT (60,0) with 2% of resonant defects: (a) Microscopic conductivity per unit of surface σ_M/C_h versus energy, (b) Electronic conductivity versus inelastic mean-free path in log scale, (c) Localization length versus energy shows $\xi < C_h$, (d) Electronic conductivity versus inelastic mean-free path, and (e) Localization length versus energy shows $\xi > C_h$.

two-dimensional system by dividing it by C_h, so $\sigma^{2D} = \frac{\sigma^{1D}}{C_h}$ is expressed in units of surface.

As shown in figure 4(c) the high concentration of resonant adsorbates leads to a plateau of minimum conductivity around $0.6\,G_0$, similar to the reported results on the 2D graphene (see figure 4(f)) in other studies [42]. This value of minimum conductivity is universal as long the diameter of zigzag SWCNT is large enough and the concentration of resonants adsorbates is high enough to actually create a dimensionality crossover in the electronic behavior.

At 2% of resonant adsorbates, figure 5 shows clearly the transition of the electronic behavior in the microscopic conductivity. For low energy in figure 5(b) the 2D scale dependent conductivity: $\sigma_{2D}\left(L_i\right) = \sigma_0 - \beta G_0 \ln\left(\frac{L_i}{l_e}\right)$, fits the decreasing behavior of the electronic conductivity towards the localization regime in the logarithmic scale for large L_i. The slope in log scale according to $\sigma_{2D}\left(L_i\right)$ shows a new universal slope, $\beta = 1/\pi$, similar to what we observe in 2D graphene [42], which confirms the 2D electronic behavior in presence of high concentration of resonant adsorbates. Based on our estimation of localization length shown in figure 5(c), this 2D electronic behavior appears when the localization length is shorter than the circumference $\xi < C_h$. For high energy as shown in figure 5(d), the 1D scale dependent conductivity confirms the 1D electronic behavior when $\xi > C_h$. Therefore the 1D/2D crossover is governed by the ratio between the localisation length ξ and the circumference C_h. Thus we can define as a function of energy within the microscopic conductivity three regimes (1)a 2D regime when $\xi < C_h$, (2) An intermediate regime when $\xi \approx C_h$ and (3) A 1D regime when $\xi > C_h$.

5. Discussion

We now discuss the case of non-resonant and resonant adsorbates by combining the results on the (60,0) nanotube and those briefly presented in the supplementary material on (30,0) and (90,0) nanotubes. We focus particularly on the localization length which is a measure of the importance of localization effects and their impact on transport. Strictly at low temperature the conductance of a nanotube becomes exponentially small if the length of the nanotube is larger than the localization length. Equivalently if this length is smaller than the localization length then the nanotube can conduct. Yet at finite temperature the inelastic scattering can destroy the localization effect on a length L_i. Therefore if τ_i is smaller than the time needed for localization τ_L the nanotube can conduct. We have discussed this in the supplementary material and find that the time needed for localization τ_L varies between 10^{-12} s and a few 10^{-11} s.

For non-resonant scatterers we find that in all cases the Anderson localization is well described by the standard 1D transport theory in a low concentration limit. This implies that the elastic mean-free path obeys the Fermi golden rule and varies inversely proportionally to the adsorbate concentrations. In addition the relation between the elastic mean-free path and the localization length obeys the Thouless relation. Depending on the Fermi energy and the adsorbate concentrations the localization length varies between 1200 nm and 30 nm. These values are similar for all three nanotubes. Yet a noticeable difference is that for smaller diameters the energy range where there are only two channels is more important. In this two channels zone the localization length tends to be
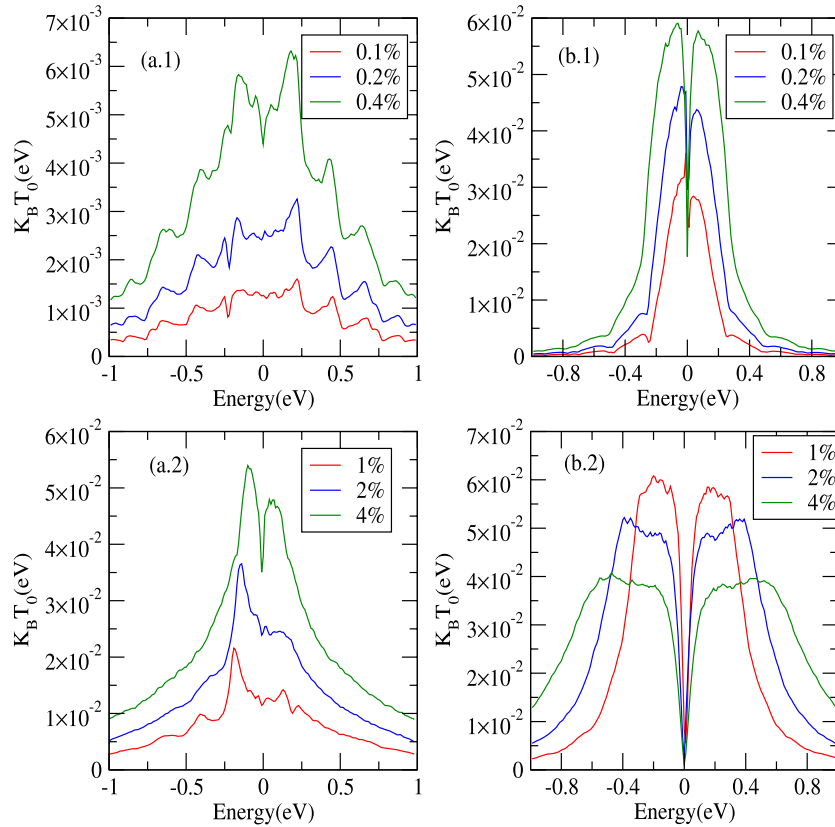
Figure 6. Temperature $k_B T_0$ as function of energy E for low and high concentrations. Results in the left column are for non-resonant defects and in the right column for resonant defects. Room temperature T_R corresponds to $k_B T_R \simeq 2.5 \times 10^{-2}$ eV.

larger than at higher energies. Therefore nanotubes with non-resonant adsorbates will present better transport when the Fermi energy is closer to the CNP.

For the resonants adsorbates the situation is opposite. Indeed the scattering matrix $T(E)$ presents a strong resonance close to the charge neutrality point and this leads to a short mean-free path and a short localization length at energies close to the charge neutrality point. Therefore in the case of resonant adsorbates the transport properties are more deteriorated close to the CNP and better transport properties will be obtained if the Fermi energy is sufficiently far from the CNP. At low concentrations the behaviour is also well described by the 1D quantum transport theory except very close to the neutrality point where even the density of states is modified by the adsorbates. However at higher concentrations and for sufficiently large diameter carbon nanotubes can behave like a 2D system and not like a 1D conductor. This happens when the elastic mean-free path and the localization length become smaller than the circumference of the nanotube. For large nanotubes with diameter of 4–5 nanometers this regime can be reached with resonant scatterers at concentrations of defects of the order of one percent and for energies of a fraction of an electron Volt away from the charge neutrality level ($E < 0.3$ eV at 2%). This 2D behaviour is comparable with the electronic behaviour in graphene, in which $\sigma(L_i)$ decreases for large L_i accordingly to the 2D scale dependent conductivity and leading to the creation of minimum microscopic conductivity around the Dirac energy. Yet at higher energies

($E > 0.5$ eV at 2%) the scattering by resonant states is less efficient and one recovers a typical 1D behaviour. Depending on energy and concentration the localization length varies between 1000 nm and 10 nm. These values are about the same in all three nanotubes.

Finally we discuss the possibility of a transport mechanism that is based on hopping. This type of transport is well documented in nanotubes and bundles or two dimensional arrays of nanotubes. At the very low temperatures of a few Kelvin, the electron-electron interaction can play a strong role but at higher temperatures the thermally activated hopping between localized states is usually due to electron-phonon coupling [47, 48]. We shortly discuss this regime now.

In the nearest neighbor hopping regime the transport is thermally activated and in the variable range hopping regime (which occurs at lower temperature) the conductivity σ is typically proportional to $\propto \exp(-(T_0/T)^{1/2})$ [49–51]. This regime of variable range hopping appears typically at temperature below $T_0 = 4/(n(E)\xi(E))$ where $\xi(E)$ is the localization length and $n(E)$ the density of states per unit length and per spin. Figure 6 shows the variation of this temperature T_0 as a function of concentration and energy E for resonant and non-resonant defects. These results show that transport through the variable range Hopping transport could occur even at room temperature in systems with sufficiently large defects concentration provided that the Fermi energy is sufficiently close to the charge neutrality point. Note that for resonant states the $T_0(E)$ decreases in the immediate vicinity of the CNP due to the

higher density of states caused by the resonant states. Around the CNP, $T_0(E)$ increases as function of concentration of resonant and non-resonant adsorbates, however beyond 1% of resonant adsorbates (at 2% and 4%) as shown in figure 6(b.2), $T_0(E)$ decreases which coincide with the appearance of the strong 2D electronic behavior previously discussed.

6. Conclusion

We have presented a study of the quantum localization in single walled carbon nanotubes (SWCNT), with resonants and non-resonants adsorbates that represent two extreme types of covalently functionalized groups with moderate and strong scattering properties. In the present study the concentration of these adsorbates varies between 0.1%, and 4% and we consider nanotubes of average and large circumferences (up to 15 nm). Our study shows that the type of adsorbates, the circumference of the nanotube and the Fermi energy are determinant for the localization phenomenon. Depending on these parameters the localization length can become small of the order of a few 10 nm. The localization can even be smaller than the circumference of the nanotube in the case where there are resonant scatterers, a Fermi energy close to the CNP and a large nanotube. In this special case the localization effect follows the 2D laws. Quite generally we find that non-resonant adsorbates have better transport properties for Fermi energy close to the CNP where it is the opposite with resonant adsorbates. These systems could also present a transport through nearest neighbor hopping or even through Variable Range Hopping even at room temperature provided that the Fermi energy is sufficiently close from the Charge Neutrality Point and also for sufficiently high concentration of adsorbates.

We believe that the present study can help to understand the localization effect in a given device and to determine in which regime it is. Therefore this work should be useful for obtaining efficient nano-sensors based on covalent functionalisation of carbon nanotubes.

ORCID iDs

Ghassen Jemaï https://orcid.org/0000-0002-7769-5192
Jouda Jemaa Khabthani https://orcid.org/0000-0003-0872-6570
Guy Trambly de Laissardière https://orcid.org/0000-0001-9065-7337
Didier Mayou https://orcid.org/0000-0003-2723-9727

References

[1] Yang L, Yu L L, Wei H W, Li W Q, Zhou X and Tian W Q 2019 Hydrogen storage of dual ti doped single-walled carbon nanotubes *Int. J. Hydrog. Energy* **44** 2960–75

[2] Muhulet A, Miculescu F, Voicu S I, Schütt F, Thakur V K and Mishra Y K 2018 Fundamentals and scopes of doped carbon nanotubes towards energy and biosensing applications *Mater. Today Energy* **9** 154–86

[3] Fu X, Xu L, Li J, Sun X and Peng H 2018 Flexible solar cells based on carbon nanomaterials *Carbon* **139** 1063–73

[4] Jeon I, Matsuo Y and Maruyama S 2018 Single walled carbon nanotubes in solar cells *Top. Curr. Chem.* **376** 4

[5] Oo T T and Debnath S 2017 Application of carbon nanotubes in perovskite solar cells: a review *AIP Conf. Proc.* **1902** 020015

[6] Yoo S M, Baek Y-K, Shin S, Kim J-H, Jung H-T, Choi Y-K and Lee S Y 2016 Single walled carbon nanotube based electrical biosensor for the label free detection of pathogenic bacteria *J. Nanosci. Nanotechnol.* **16** 6520–5

[7] Choi H-K, Lee J, Park M-K and Oh J-H 2017 Development of single-walled carbon nanotube-based biosensor for the detection of staphylococcus aureus *J. Food Qual.* **2017** 11

[8] Britz D A and Khlobystov A N 2006 Noncovalent interactions of molecules with single walled carbon nanotubes *Chem. Soc. Rev.* **35** 637–59

[9] Khan W, Sharma R and Saini P 2016 Chapter: Carbon nanotube-based polymer composites P, properties and applications *Carbon Nanotubes—Current Progress of their Polymer Composites* (InTech)

[10] Kamran U, Heo Y-J, Lee J W and Park S-J 2019 Functionalized carbon materials for electronic devices: a review *Micromachines* **10** 234

[11] Zhu Z 2017 An overview of carbon nanotubes and graphene for biosensing applications *Nano-Micro Lett.* **9** 25

[12] Zaporotskova I V, Boroznina N P, Parkhomenko Y N and Kozhitov L V 2016 Carbon nanotubes: sensor properties. A review *Mod. Electron. Mater.* **2** 95–105

[13] Gómez-Navarro C, Pablo P J D, Gómez-Herrero J, Biel B, Garcia-Vidal F J, Rubio A and Flores F 2005 Tuning the conductance of single-walled carbon nanotubes by ion irradiation in the anderson localization regime *Nat. Mater.* **4** 534

[14] Flores F, Biel B, Rubio A, Garcia-Vidal F J, Gomez-Navarro C, de Pablo P and Gomez-Herrero J 2008 Anderson localization regime in carbon nanotubes: size dependent properties *J. Phys.: Condens. Matter* **20** 304211

[15] Latil S, Roche S, Mayou D and Charlier J-C 2004 Mesoscopic transport in chemically doped carbon nanotubes *Phys. Rev. Lett.* **92** 256805

[16] Latil S, Roche S and Charlier J-C 2005 Electronic transport in carbon nanotubes with random coverage of physisorbed molecules *Nano Lett.* **5** 2216–9

[17] Ishii H, Roche S, Kobayashi N and Hirose K 2010 Inelastic transport in vibrating disordered carbon nanotubes: scattering times and temperature-dependent decoherence effects *Phys. Rev. Lett.* **104** 116801

[18] McEuen P L, Bockrath M, Cobden D H, Yoon Y-G and Louie S G 1999 Disorder, pseudospins, and backscattering in carbon nanotubes *Phys. Rev. Lett.* **83** 5098–101

[19] McEuen P L and Park J-Y 2004 Electron transport in single walled carbon nanotubes *MRS Bull.* **29** 272–5

[20] Li Z, Wang C-Y, Ke S-H and Yang W 2009 First-principles study for transport properties of defective carbon nanotubes with oxygen adsorption *Eur. Phys. J.* B **69** 375–82

[21] López-Bezanilla A, Triozon F, Latil S, Blase X and Roche S 2009 Effect of the chemical functionalization on charge transport in carbon nanotubes at the mesoscopic scale *Nano Lett.* **9** 940–4

[22] Khoeini F, Shokri A and Farman H 2009 Electronic transport through superlattice-like disordered carbon nanotubes *Solid State Commun.* **149** 874–9

[23] Zienert A, Schuster J and Gessner T 2013 Comparison of quantum mechanical methods for the simulation of electronic transport through carbon nanotubes *Microelectron. Eng.* **106** 100–5

[24] Teichert F, Zienert A, Schuster J and Schreiber M 2014 Strong localization in defective carbon nanotubes: a recursive Green's function study *New J. Phys.* **16** 123026

[25] Teichert F, Zienert A, Schuster J and Schreiber M 2017 Electronic transport in metallic carbon nanotubes with mixed defects within the strong localization regime *Comput. Mater. Sci.* **138** 49–57

[26] Lopez-Bezanilla A, Froufe-Pérez L S, Roche S and Sáenz J J 2018 Unequivocal signatures of the crossover to anderson localization in realistic models of disordered quasi-one-dimensional materials *Phys. Rev.* B **98** 235423

[27] Anderson P W 1958 Absence of diffusion in certain random lattices *Phys. Rev.* **109** 1492–505

[28] Thouless D J 1970 Anderson's theory of localized states *J. Phys. C: Solid State Phys.* **3** 1559

[29] Thouless D J 1973 Localization distance and mean free path in one-dimensional disordered systems *J. Phys. C: Solid State Phys.* **6** L49

[30] Saito R 1998 *Physical Properties of Carbon NanotubesHardcover* 1st edn (Singapore: World Scientific)

[31] Pereira V M, Lopes dos Santos J M B and Castro Neto A H 2008 Modeling disorder in graphene *Phys. Rev.* B **77** 115109

[32] Setaro A *et al* 2017 Preserving p-conjugation in covalently functionalized carbon nanotubes for optoelectronic applications *Nat. Commun.* **8** 14281

[33] Fan Z, Uppstu A and Harju A 2014 Anderson localization in two-dimensional graphene with short-range disorder: one-parameter scaling and finite-size effects *Phys. Rev.* B **89** 245422

[34] Uppstu A, Fan Z and Harju A 2014 Obtaining localization properties efficiently using the Kubo–Greenwood formalism *Phys. Rev.* B **89** 075420

[35] Fan Z, Uppstu A, Siro T and Harju A 2014 Efficient linear-scaling quantum transport calculations on graphics processing units and applications on electron transport in graphene *Comput. Phys. Commun.* **185** 28–39

[36] Mayou D 1988 Calculation of the conductivity in the short mean free path regime *Europhys. Lett.* **6** 549–54

[37] Mayou D and Khanna S N 1995 A real space approach to electronic transport *J. de Phys.* I **5** 1199–211

[38] Roche S and Mayou D 1997 Conductivity of quasiperiodic systems: a numerical study *Phys. Rev. Lett.* **79** 2518–21

[39] Roche S and Mayou D 1999 Formalism for the computation of the rkky interaction in aperiodic systems *Phys. Rev.* B **60** 322–8

[40] Triozon F, Vidal J, Mosseri R and Mayou D 2002 Quantum dynamics in two- and three-dimensional quasiperiodic tilings *Phys. Rev.* B **65** 220202

[41] Mayou D and Trambly de Laissardi G 2008 Chapter 7 quantum transport in quasicrystals and complex metallic alloys *Quasicrystals* (*Handbook of Metal Physics* vol 3) ed T Fujiwara and Ishii Y (Amsterdam: Elsevier) pp 209–65

[42] Trambly de Laissardi G and Mayou D 2013 Conductivity of graphene with resonant and nonresonant adsorbates *Phys. Rev. Lett.* **111** 146601

[43] Missaoui A, Khabthani J J, Jaidane N-E, Mayou D and Trambly de Laissardi G 2018 Mobility gap and quantum transport in functionalized graphene bilayer *J. Phys.: Condens. Matter* **30** 195701

[44] Missaoui A, Khabthani J J, Jaidane N-E, Mayou D and Trambly de Laissardi G 2017 Numerical analysis of electronic conductivity in graphene with resonant adsorbates: comparison of monolayer and bernal bilayer *Eur. Phys. J.* B **90** 75

[45] Lee P A and Ramakrishnan T V 1985 Disordered electronic systems *Rev. Mod. Phys.* **57** 287–337

[46] Beenakker C W J 1997 Random-matrix theory of quantum transport *Rev. Mod. Phys.* **69** 731–808

[47] Roche S, Jiang J, Torres L E F F and Saito R 2007 Charge transport in carbon nanotubes: quantum effects of electron–phonon coupling *J. Phys.: Condens. Matter* **19** 183203

[48] Bo Xu J Y and Liu Z 2013 Chapter: Phonon scattering and electron transport in single wall carbon nanotube *Physical and Chemical Properties of Carbon Nanotubes* (InTech)

[49] Yu Z G and Song X 2001 Variable range hopping and electrical conductivity along the dna double helix *Phys. Rev. Lett.* **86** 6018–21

[50] Wang D P, Feldman D E, Perkins B R, Yin A J, Wang G H, Xu J M and Zaslavsky A 2007 Hopping conduction in disordered carbon nanotubes *Solid State Commun.* **142** 287–91

[51] Pipinys P and Kiveris A 2012 Variable range hopping and/or phonon-assisted tunneling mechanism of electronic transport in polymers and carbon nanotubes *Cent. Eur. J. Phys.* **10** 271–81